

1 Ensemble streamflow prediction considering the influence of 2 reservoirs in Narmada River basin, India

3
4 Urmin Vegad¹ and Vimal Mishra^{1,2*}

5
6 ¹Civil Engineering, Indian Institute of Technology (IIT) Gandhinagar

7 ²Earth Sciences, Indian Institute of Technology (IIT) Gandhinagar

8 *Corresponding author: vmishra@iitgn.ac.in

9 Abstract

10 Developing an ensemble hydrological prediction system is essential for reservoir operations and flood early
11 warning. However, efforts to build hydrological ensemble prediction systems considering the influence of
12 reservoirs have been lacking in India. We examine the potential of the Extended Range Forecast System (ERFS,
13 16 ensemble members) and Global Ensemble Forecast System (GEFS, 21 ensemble members) forecast for
14 streamflow prediction in India using the Narmada River basin as a testbed. We use the Variable Infiltration
15 Capacity (VIC) with reservoir operations (VIC-Res) scheme to simulate the daily river flow at four locations in
16 the Narmada basin. Streamflow prediction skills of the ERFS forecast were examined for the period 2003-2018 at
17 1-32 day lead. We compared the streamflow forecast skills of raw meteorological forecasts from ERFS and GEFS
18 at a 1-10 day lead for the summer monsoon (June-September) 2019-2020. The ERFS forecast underestimates
19 extreme precipitation against the observations compared to the GEFS forecast during the summer monsoon of
20 2019-2020. However, both the forecast products show better skills for minimum and maximum temperatures than
21 precipitation. Ensemble streamflow forecast from the GEFS performs better than the ERFS during 2019-2020.
22 The performance of GEFS based ensemble streamflow forecast declines after five days lead. Overall, the GEFS
23 ensemble streamflow forecast can provide reliable skills at a 1-5 day lead, which can be utilized in streamflow
24 prediction. Our findings provide directions for developing a flood early warning system based on ensemble
25 streamflow prediction considering the influence of reservoirs in India.

Deleted: hydrologic

Deleted: hydrologic

26 1. Introduction

27 Floods are one of India's most destructive and frequently occurring natural disasters. Floods accounted for about
28 47% of natural disasters in India during the last 100 years (Tripathi, 2016). Riverine floods occur during the
29 summer monsoon season affecting approximately five million people annually (Luo et al., 2015). Singh and Kumar
30 (2013) reported an increase in the frequency of floods in India. About 20% of the total flood-prone area gets
31 affected every year (Ray et al., 2019). Floods in 2018 caused an economic loss of more than twelve billion dollars

Deleted: In India, the frequency of floods has increased in the past

36 (USD) and resulted in the loss of 1808 lives (Joshi, 2020). In addition, climate warming is projected to increase
37 the frequency and intensity of riverine floods (Field et al., 2011; Luo et al., 2015; Nanditha and Mishra, 2022; Ali
38 et al., 2019).

39
40 Preparedness for disasters like floods can help in mitigating economic loss and reducing flood mortality (Jain et
41 al., 2018). While losses due to floods are projected to rise under the warming climate, human mortality can be
42 reduced with flood early warning systems and effective communication (Dipti, 2017, Nanditha and Mishra, 2021).
43 Therefore, developing a robust flood prediction system is necessary for early warning and preparedness.
44 Streamflow prediction is an essential component of flood forecasting, which helps in planning and decision-
45 making (Georgakakos et al., 2012; Alfieri et al., 2013). Most of the streamflow prediction systems in India are
46 based on the deterministic approach (Harsha, 2020a; Todini, 2017, Nanditha and Mishra, 2021), which do not
47 account for perturbations in initial conditions to quantify the uncertainty (Bowler et al., 2008). Uncertainty
48 quantification in streamflow prediction can reduce the risk of false alarms based on deterministic forecast (Todini,
49 2017). In addition, ensemble streamflow prediction is essential for the probabilistic flood forecast. The
50 probabilistic approach performs better than the deterministic approach by quantifying uncertainties associated with
51 flood prediction and early warning system (Krzysztofowicz, 2001). Previous studies used ensemble streamflow
52 prediction in flood forecasting (Cloke and Pappenberger, 2009; Wu et al., 2020) using ensemble meteorological
53 forecast and hydrological models (Zhang et al., 2020). Ensemble weather forecast provides multiple members at
54 the same location and time that can be used for probabilistic hydrological prediction. However, several challenges
55 are associated with the operational ensemble streamflow forecast, including computational limitations, explanation
56 of ensemble forecasts to non-experts, and up-gradation in the policy to use the forecast for decision making
57 (Demeritt et al., 2010; Arnal et al., 2020). Despite these challenges, ensemble flood forecasts consider the
58 uncertainty that can be used for preparedness and planning compared to the deterministic forecast approach.
59 (Pappenberger et al., 2012; Cloke and Pappenberger, 2009).

60
61 Indian river basins are considerably affected by human interventions including presence of reservoirs, water
62 withdrawal for irrigation, and inter/intra basin water transfer (Nanditha and Mishra, 2021; Madhusoodhanan et al.,
63 2016; Gosain et al., 2006). India has more than 5000 large dams while about 450 are currently under construction
64 (NRLD, 2017). Reservoirs and irrigation can considerably modulate terrestrial water and energy budgets in India
65 (Shah et al., 2019). For instance, Shah et al. (2019) showed that evapotranspiration and latent heat flux are
66 increased under the presence of irrigation and reservoirs in Indian river basins compared to their natural conditions.
67 Dong et al. (2022) reported that reservoirs can significantly (~ 25%) contribute to the variation of terrestrial water
68 storage in China. In addition, the presence of reservoirs can considerably affect streamflow variability in the
69 downstream regions (Zajac et al., 2017; Yun et al., 2020; Chai et al., 2019). Reservoirs in India are multipurpose
70 as these store water for the dry season, generate hydropower, and attenuate floods in the downstream regions
71 (Tiwari and Mishra, 2022). Reservoirs store water during the summer monsoon season and release water during

Deleted: hydrologic

Deleted: hydrologic

74 the dry season for irrigation. Similarly, based on the reservoir rule curve, a buffer storage is kept during the wet
75 season to accommodate high inflow so that flood risk can be minimized in the downstream region. Therefore,
76 there are several challenges associated with the streamflow forecast in the river basins that are affected by
77 reservoirs. Most often hydrological model-based flood/streamflow forecast does not consider the influence of
78 reservoirs that could lead to under or overestimation of flow depending on the season (Nanditha and Mishra, 2021;
79 Dang et al., 2019). Incorporating reservoir influence in **hydrological** models is essential as reservoirs significantly
80 affect the magnitude and timing of streamflow (Zajac et al., 2017; Yassin et al., 2019; Dang et al., 2019). Several
81 efforts have been made to incorporate the influence of reservoirs in the **hydrological** models (Boulangue Julien and
82 Hanasaki Naota, 2013; Dang et al., 2019; Hanasaki et al., 2018). However, most of the previous studies on flood
83 forecasts and early warnings in India did not consider the influence of reservoirs (Goswami et al., 2018; Sikder
84 and Hossain, 2019).

Deleted: hydrologic

Deleted: hydrologic

85
86 The Central Water Commission (CWC) manages flood forecast systems in India. The flood forecast network
87 monitors 325 stations across India. CWC observes real-time water level and discharge along the major rivers of
88 India during the designated flood period. The flood forecast is performed using statistical correlation methods
89 from gauge to gauge. Moreover, Quantitative Precipitation Forecast (QPF) from the India Meteorological
90 Department (IMD) is used to forecast floods at a 3-day lead time (Teja and Umamahesh, 2020). The current model-
91 based flood forecast approach used by CWC is deterministic, which lacks incorporating uncertainties in the
92 forecast and early warning system. An ensemble forecast system can help in flood early warning and decision-
93 making (Harsha, 2020b; Nanditha and Mishra, 2021). Various ensemble forecast products are available from the
94 India Meteorological Department (IMD) and the Indian Institute of Tropical Meteorology (IITM). However, the
95 utility of these forecast products for streamflow prediction and flood early warning at the river basin scale has not
96 been examined. In addition, despite the advantages of ensemble **hydrological** prediction, India's current
97 **hydrological** forecast systems are mainly deterministic. Given the increasing flood damage in India, the
98 overarching aim of this work is to explore the utility of ensemble forecast products for streamflow prediction in
99 India. We considered the Narmada River basin as a testbed to examine the potential of ensemble **hydrological**
100 prediction. We used the Variable Infiltration Capacity (VIC) with reservoir operations (VIC-Res) scheme, which
101 incorporates the effect of reservoirs (Dang et al., 2019). Extended Range Forecast System (ERFS) and Global
102 Ensemble Forecast System (GEFS) ensemble forecasts developed by IITM are used to examine the **hydrological**
103 prediction skills at the selected gauge stations in the Narmada basin.

Deleted: hydrologic

Deleted: hydrologic

Deleted: hydrologic

Deleted: hydrologic

105 2. Data and methods

106 2.1 Study region and datasets

107 Narmada is the fifth biggest and the largest west-flowing river in India. The Narmada river basin falls in two states,
108 Gujarat and Madhya Pradesh. Many tributaries contribute to the river through its way to the Arabian Sea, with the

115 Tawa river being its longest tributary. The catchment area of the river basin at the outlet is approximately 98,796
 116 km². The upper portion of the basin falls in Madhya Pradesh. The mean annual rainfall in the Narmada basin is
 117 1064 mm. Most of the total annual precipitation occurs during the summer monsoon season (June-September).
 118 We used observed daily streamflow at four stations: Sandia, Handia, Mandleshwar, and Garudeshwar (Fig. 1).
 119 There are several ongoing hydropower and irrigation projects in the Narmada basin. Our **hydrological** modelling
 120 framework has considered four dams: Bargi, Tawa, Indira Sagar, and Sardar Sarovar (Table 1). Bargi and Tawa
 121 reservoirs were primarily constructed for irrigation purposes (Table 1). At the same time, Indira Sagar (0.975
 122 Billion Cubic Meters (BCM)) and Sardar Sarovar (5.8 BCM) are the two largest reservoirs that are used for multi-
 123 purpose.

Deleted: hydrologic

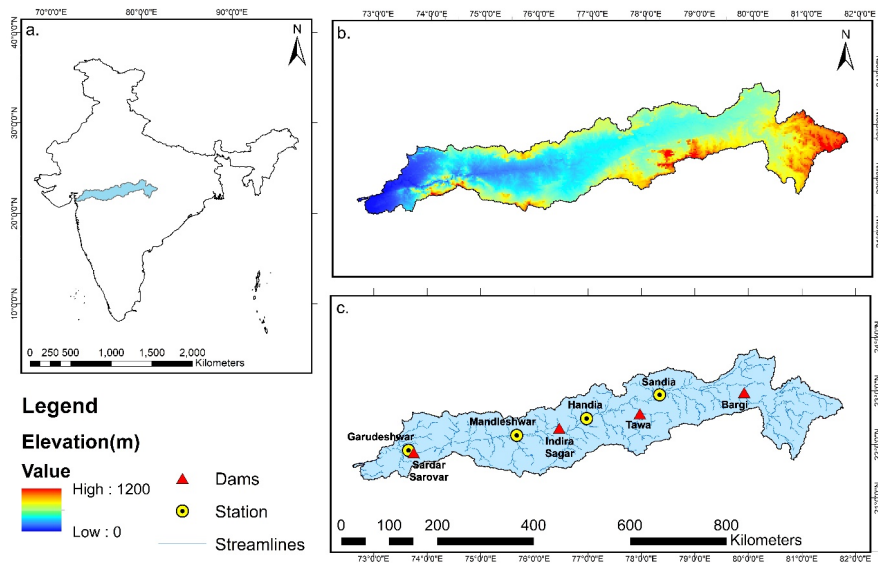
124 **Table 1. Parameters of reservoirs that were considered in **hydrological** simulations**

Deleted: hydrologic

Sr No	Name of dam	Year of completion	Height above lower foundation (m)	Length of dam (m)	Gross storage capacity (BCM)	Effective storage capacity (BCM)
1	Bargi	1988	69.8	5357	3.92	3.18
2	Tawa	1978	57.92	1944.92	2.312	1.94
3	Indira Sagar	2006	91.4	654	12.22	9.75
4	Sardar Sarovar	2017	163	1210	9.5	5.8

Formatted Table

125



128

129 **Figure 1. Basic information about (a) location in India, (b) topography, c) streamlines, location of streamflow gauge**
 130 **stations and reservoirs**

131 We used 0.25° (approximate spatial resolution; ~27.5 x 27.5 km) gridded daily precipitation from IMD for the
 132 1951-2020 period (Pai et al., 2014). The daily gridded precipitation product is developed using observations from
 133 6955 rain gauge stations (Pai et al., 2015). Pai et al. (2015) examined daily rainfall trends, long-term climatology,
 134 and variability over the central Indian region. The high resolution (0.25°) gridded precipitation captures spatial
 135 variability in better manner compared to previous coarse-gridded rainfall products. We obtained daily 1° gridded
 136 maximum and minimum temperatures from IMD (Srivastava et al., 2009). Srivastava et al. (2009) developed the
 137 gridded temperature dataset using observations from 395 stations. We used bilinear interpolation to convert the 1°
 138 gridded temperature to 0.25° resolution to make it consistent with the gridded precipitation. The VIC model also
 139 requires daily wind speed as an input. We obtained the wind speed from the National Centers for Environmental
 140 Prediction (NCEP)-National Centers for Atmospheric Research (NCAR)
 141 (<https://psl.noaa.gov/data/gridded/data.ncep.reanalysis.pressure.html>). The wind speed at a coarser (1.875° x
 142 1.905°) resolution was interpolated using bilinear interpolation to 0.25° to make it consistent with the other
 143 meteorological datasets. The VIC model's vegetation parameters were obtained from the Advanced Very High-
 144 Resolution Radiometer (AVHRR) global land cover, which is available at 1-km spatial resolution (Sheffield and
 145 Wood, 2007). Soil parameters at 0.25° were developed using the Harmonized World Soil Database (HWSD
 146 version 1.2) [Gao et al., 2009]. We used digital elevation model data from Shuttle Radar Topography Mission

147 (SRTM) at 90 m spatial resolution (Jarvis, 2008). The hydrological model considers sub-grid variability of
148 topography and vegetation (Gao et al. 2010). Therefore, the high-resolution vegetation and elevation datasets were
149 used to extract values for different tiles within a grid.

150 We obtained observed daily streamflow, reservoir water level, and reservoir live storage data from the India -
151 Water Resources Information System (IWRIS; <http://www.indiawris.gov.in>), which is a joint venture of the
152 Central Water Commission, the Ministry of Jal Shakti, and the Indian Space Research Organization (ISRO).
153 Streamflow and reservoir levels are monitored at various locations in the Narmada basin by CWC. We selected
154 the gauge stations (Sandia, Handia, Mandleshwar, and Garudeshwar) that have observed flow data for at least 15
155 years. The reservoir storage and water level data were obtained for different periods depending on the data
156 availability.

157 We obtained the Extended Range Forecast System (ERFS) meteorological forecast for the 2003-2020 period. In
158 addition, the Global Ensemble Forecast System (GEFS) meteorological forecast was obtained for the summer
159 monsoon season (July-September) of 2019-2020 from the IITM. Both the ERFS and GEFS forecast products are
160 developed at IITM and are currently being used for the operational weather forecast by the IMD. In June 2018,
161 the high-resolution GEFS forecast was developed and then transferred to the IMD for operational forecasting
162 (Mukhopadhyay et al., 2018). The GEFS dataset has a horizontal resolution of T1534 (~12.5 km) and consists of
163 21 ensemble members (one control and twenty perturbed). The dynamic core of the model is based on semi-
164 Lagrangian framework, which reduces considerable computational requirements. The initial conditions (ICs) for
165 meteorological forecasts are obtained from Global Data Assimilation System (GDAS). The GEFS is being run
166 operationally for the ten-day lead forecast using daily Initial Conditions (ICs) during the summer monsoon period.
167 The GEFS forecast successfully predicted the 2018 Kerala extreme rainfall at 2-3 days lead and showed reasonable
168 forecast skills at 5-7 days lead (Mukhopadhyay et al., 2018).

169 The ERFS multi-model system consists of four (CFSv2T382, CFSv2T126, GFSbcT382 and GFSbcT126) suites,
170 each having four ensemble members (one control and three perturbed). Therefore, sixteen ensemble members are
171 available for the ERFS forecast. The model is being run operationally for 32 days lead based on the initial
172 conditions of every Wednesday. Atmospheric and oceanic initial conditions from the National Center for Medium-
173 Range Weather Forecasting (NCMWRP) and Indian National Centre for Ocean Information Services (INCOSIS)
174 assimilation system are used by the models in ERFS. We used the sixteen ensemble meteorological forecasts to
175 simulate the daily streamflow at 1-32 days leads at selected stations in the Narmada river basin. Shah et al. (2017)
176 reported that ERFS performed better than the Global Ensemble Forecast System v2 (GEFSv2) and Climate
177 Forecast System v2 (CFSv2) in precipitation forecast during the summer monsoon season over India.

178 2.2 The VIC-Res hydrological model

Deleted: hydrologic

Deleted: hydrologic

180 We used the VIC-Res [hydrological](#) model (Dang et al., 2019), a novel variant of the VIC model (Liang et al.,
181 1994), to simulate streamflow. A combination of the VIC model and the routing model developed by Dang et al.
182 (2019) was used to simulate streamflow at the selected locations in the basin. Dang et al. (2019) incorporated the
183 effect of reservoirs by considering the reservoir storage dynamics and operating rules within the streamflow
184 routing model in the VIC-Res model. The rainfall-runoff model generates water and energy fluxes within each
185 grid using climate forcing, soil parameters, land use/land cover, and the digital elevation model. The model uses
186 vegetation cover for each tile and three soil layers for each grid cell. The upper two soil layers control runoff,
187 infiltration, and evaporation, while the bottom layer governs baseflow. The routing model uses water fluxes (runoff
188 and baseflow) from each grid to simulate streamflow at selected gauge stations using the linearized Saint-Venant
189 equations. The routing model uses flow direction, fractional area within a grid, and station location as input to
190 generate streamflow. In addition, the VIC-Res model requires reservoir parameters and location as inputs. The
191 reservoir parameters include full reservoir level (FRL), dead water level, storage capacity, dead storage, rated
192 head, and the year when reservoir became operational. The VIC-Res considers a grid as a reservoir and the
193 incoming streamflow to that reservoir is considered as the inflow. In addition to the reservoir parameters, observed
194 seasonal cycle is also required as input to the routing scheme. The model implements mass balance equation at
195 each time step to calculate storage and outflow/release from the reservoir. The VIC-Res model simulates daily
196 reservoir inflow, outflow, live storage, and water level. Dang et al. (2019) reported that even the model without a
197 reservoir exhibits almost the same level of accuracy. However, as the parametrization is inappropriate when the
198 model is calibrated using the observed flow that is affected by reservoirs, hydrological processes simulated by the
199 model can be erroneous.

200 We used observed daily precipitation, maximum and minimum temperatures from IMD, and wind speed from
201 NCEP-NCAR reanalysis as meteorological forcing. We used reservoir storage observations to input the seasonal
202 cycle for each reservoir into the model. An autocalibration module developed by Dang et al. (2020) was used to
203 calibrate soil parameters of the VIC-Res model for the Narmada River basin. The autocalibration module uses the
204 ϵ -NSGAI multi-objective evolutionary algorithm (Reed et al., 2013) to adjust the values of sensitive soil
205 parameters. The autocalibration module can be used to calibrate model parameters at the outlet of different sub-
206 basins within a river basin. First, we used autocalibration to calibrate parameters of upstream basins, then the
207 parameters for the downstream basins were calibrated for the grids that are not part of the upstream basins. We
208 used five soil parameters (B_{inf} , D_s , D_{smax} , W_s , and depth of three soil layers) to calibrate daily streamflow at the
209 selected gauge stations in the basin as described in Mishra et al. (2010). B_{inf} is the variable infiltration curve
210 parameter. D_{smax} is the maximum velocity of baseflow. D_s is a fraction of D_{smax} where non-linear baseflow begins.
211 W_s is a fraction of maximum soil moisture non-linear baseflow occurs (Liang et al., 1994). Further details of the
212 calibration parameters can be obtained from Mishra et al. (2010). The autocalibration module optimizes the
213 model's performance in simulating streamflow at selected stations considering reservoir dynamics. We set our
214 objective to maximize Nash-Sutcliffe Efficiency (NSE) [Dawson et al., 2007; Nash and Sutcliffe, 1970]. The
215 model performance was evaluated for daily streamflow, the water level of reservoirs, and the live storage of

217 reservoirs using NSE and coefficient of determination (R^2). Daily streamflow was calibrated and evaluated at
218 Sandia, Handia, Mandleshwar, and Garudeshwar. We selected different periods for the calibration and evaluation
219 of the VIC-Res model based on the availability of observed streamflow. For instance, we selected the years 1986-
220 2000, 1986-2000, 1998-2005, 1998-2005 as the calibration period, while the years 2001-2018, 2001-2018, 2015-
221 2018, 2015-2018 as the evaluation period for stations Sandia, Handia, Mandleshwar, and Garudeshwar,
222 respectively. The VIC-Res model performance was also evaluated against water level and live storage for Bargi,
223 Tawa, Indira Sagar, and Sardar Sarovar reservoirs.

224 We first generated daily meteorological forcing of both ERFs and GEFS forecasts. The ERFs forecast is available
225 for the extended range (1-32 day lead), while the GEFS forecast is available at 1-10 day lead. We developed
226 observed initial conditions for each forecast date by forcing the long-term (20 years) observed meteorological
227 forcing from IMD into the calibrated VIC-Res model. Therefore, the model spin-up is considered in the observed
228 initial state. We simulated a daily streamflow forecast at all the four selected gauge stations using the
229 meteorological forcing and initial conditions. The VIC-Res simulations were run for all the ensemble members
230 for ERFs and GEFS forecasts. The ensemble streamflow forecasts were simulated for 1-32 days lead and ten days
231 lead for ERFs and GEFS datasets. The ERFs forecast simulations were run for 1-32 days lead with the initial
232 conditions of every Wednesday generated from VIC-Res model using the observed forcings. Similarly, GEFS
233 streamflow forecast simulations were performed for 1-10 days lead with initial conditions one day before the
234 forecast.

235 2.3 Forecast skill evaluation

236 We evaluated the skills of the streamflow forecast generated using the ERFs and GEFS meteorological forecast
237 by comparing the simulated streamflow forecast to the observed daily streamflow at each of the four locations.
238 The model simulated streamflow forecast was evaluated against the VIC-Res model simulated daily streamflow
239 using the observed forcing due to the unavailability of the observed streamflow for the years 2019-2020. The
240 ERFs meteorological forcing was used to run the VIC-Res model for 1-32 days from each forecast date using the
241 initial condition generated using the observed forcing from IMD. Similarly, we ran the GEFS ensemble members
242 for a 1-10 days lead for each forecast date. We used bias and Normalized Root Mean Square Error (NRMSE) to
243 evaluate the performance of individual ensemble forecast members, which can be estimated as follows:

$$Bias = \sum_{i=1}^n (Q_i - Q_{obs,i}) \quad (1)$$

$$NRMSE = \frac{RMSE}{O} \quad (2)$$

where, \bar{O} = mean of observations.

$$RMSE = \sqrt{\frac{\sum_{i=1}^n (Q_{i,i} - Q_{obs,i})^2}{n}} \quad (3)$$

244 where $Q_{obs,i}$ and $Q_{sim,i}$ are observed and simulated streamflow, respectively. Bias provides a measure of
245 correspondence between the mean of observations and the mean of the VIC-Res model simulations, while NRMSE
246 represents the relative magnitude of the squared error. We also evaluated the skills of ERFs forecast using
247 Continuous Ranked Probability Score (CRPS) [Hersbach, 2000], which measures the closeness between the
248 distributions of forecast and observations. The CPRS can be estimated as follows:

$$249 \quad CRPS(F, x) = \int_{-\infty}^{\infty} (F(y) - H(y - x))^2 dy \quad (4)$$

250 where F(x) is the cumulative distribution function (CDF) associated with probabilistic forecast and H(x) is the
251 Heaviside function ($H(x) = 1$ for $x \geq 0$ and zero otherwise). The unit of CRPS is the same the of observations.
252 Gneiting and Raftery (2007) suggested CPRS as a direct measure to compare deterministic and probabilistic
253 forecasts.

254 3 Results

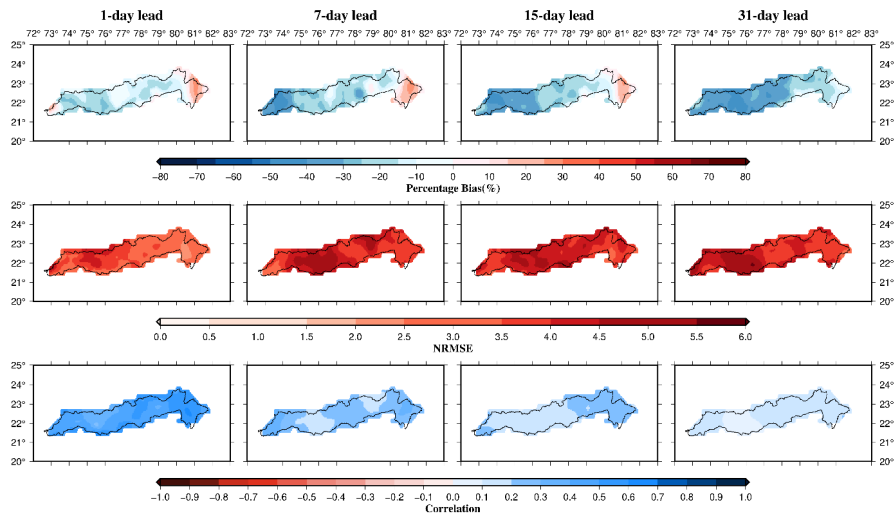
255 3.1 Skill evaluation of ERFs and GEFS meteorological forecasts

256 First, we evaluated ERFs precipitation and temperature forecast skills for 1-, 7-, 15-, and 31-day leads. We used
257 bias, NRMSE, and correlation coefficient (r) to estimate the forecast skills. The forecast skill was evaluated for
258 the period 2003-2018. We estimated the forecast skill for each ensemble member and then calculated the median
259 of the forecast skill of all the sixteen members for each grid in the Narmada river basin. Precipitation forecast from
260 ERFs shows a negative bias indicating an underestimation compared to observed rainfall. The dry bias in
261 precipitation forecast increases with the lead time (Fig. 2). For the 1-day lead, precipitation forecast from ERFs
262 showed a moderate positive correlation (median ~ 0.49), which declines with the lead time. Similarly, NRMSE in
263 precipitation forecast is large (>2.0) over the river basin. We also estimated bias in the precipitation forecast
264 exceeding the 90th percentile (Fig. 3). The extreme rainfall in the raw ERFs forecast dataset exhibited a weaker
265 correlation with the observed extreme precipitation. Moreover, a considerable dry bias in the extreme precipitation
266 forecast was found. We also evaluated forecast skills for maximum and minimum temperature against the observed
267 temperatures from IMD for the 2003-2018 period (Fig. S1 and S2). The daily temperature forecast showed a
268 relatively higher positive correlation with the observed temperatures from IMD. Moreover, lower NRMSE was

Deleted: P_{obs}

Deleted: P_{sim}

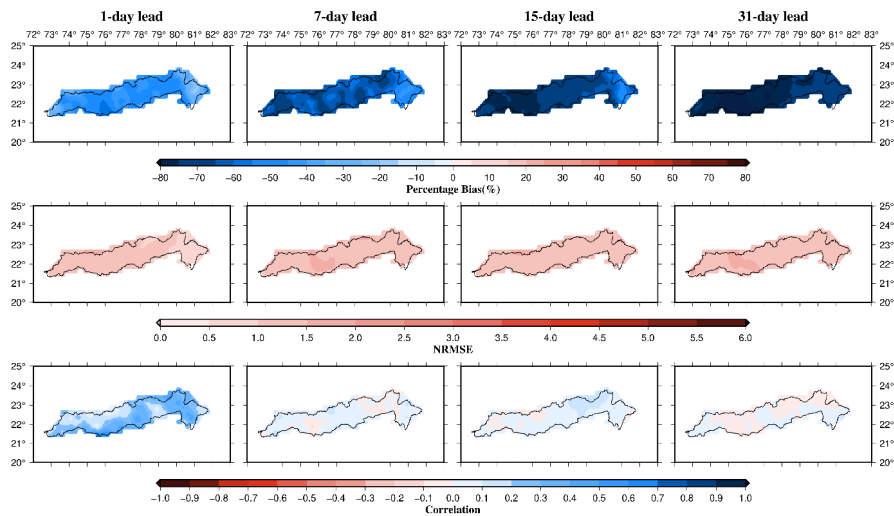
271 noted for the temperature forecast than the observed maximum and minimum temperatures. However, a positive
272 bias of ~ 1.5 °C (median of all grids in the basin) was found in minimum temperature forecast at all the lead times.



273

274 **Figure 2. Evaluation of ERFS precipitation forecast against observations for the 2003-2018 period. Forecast skills**
275 **were evaluated using bias, NRMSE, and correlation for each ensemble member and the median skill is presented.**

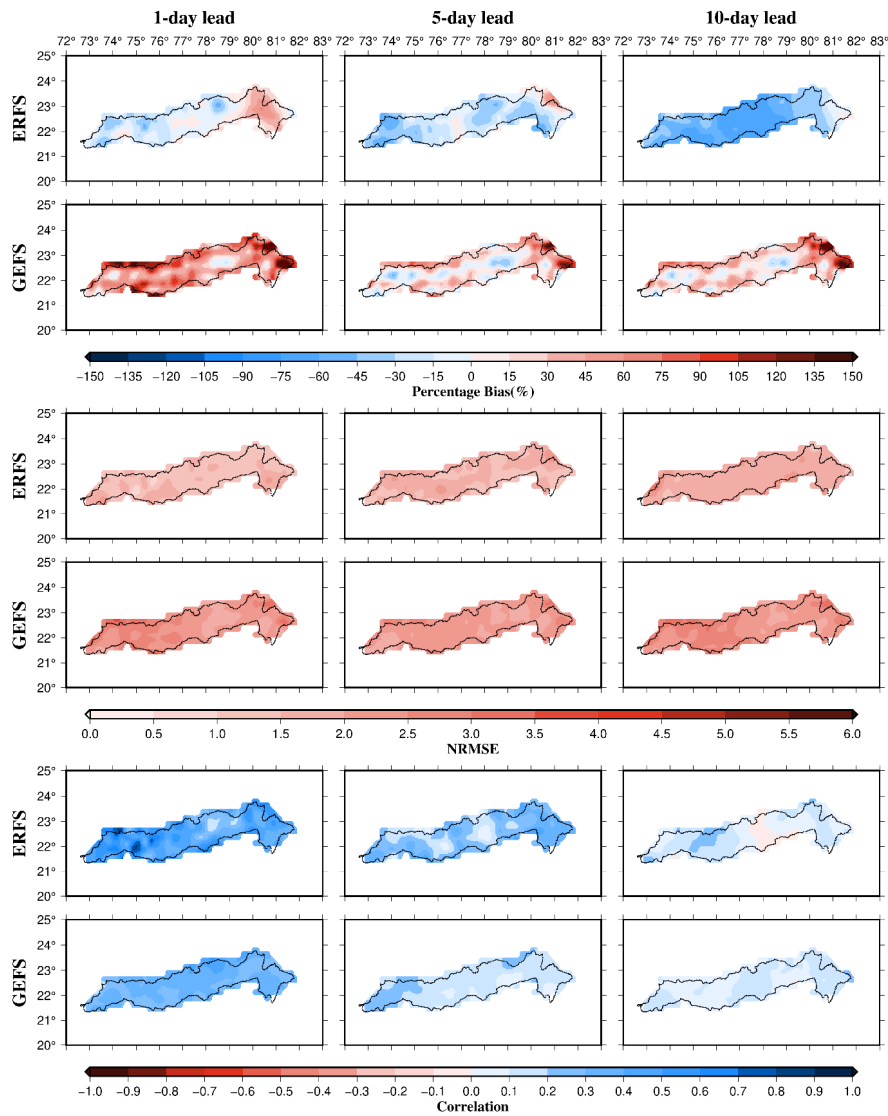
276



277

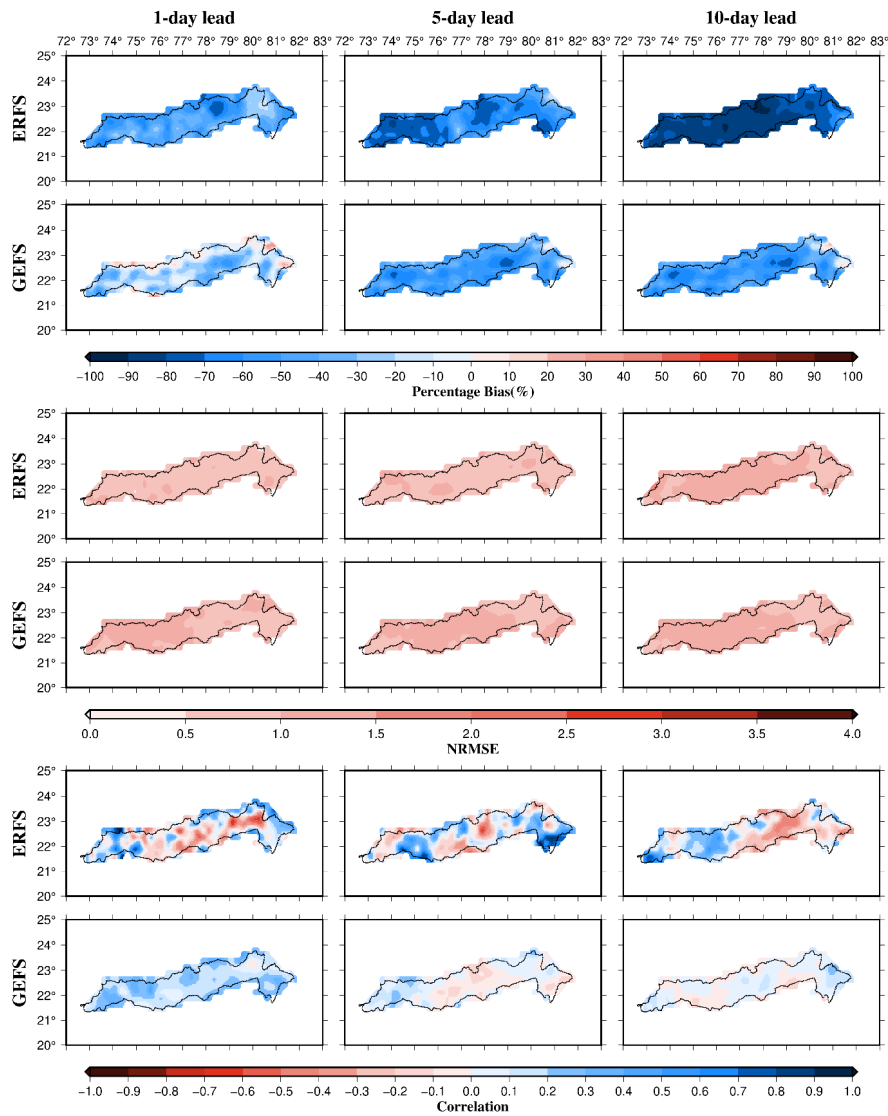
278 **Figure 3, Evaluation of extreme precipitation (>90th percentile) forecast skill from ERFs for the 2003-2018 period.**
 279 **Forecast skills were evaluated using bias, NRMSE, and correlation for each ensemble member and the median skill is**
 280 **presented.**

281 Next, we compared the ERFs and GEFS ensemble forecast skills for the summer monsoon (June-September) of
 282 the 2019-2020 period. We limit the comparison to the two years as the GEFS ensemble forecast is available only
 283 for 2019-2020. We evaluated forecast skills for 1-, 5-, and 10-day leads (Fig. 4). Our results show that the ERFs
 284 precipitation forecast has a dry bias across the river basin and all the leads (Fig 4). The GEFS precipitation forecast
 285 showed a positive (wet) bias in the majority of the Narmada river basin. The forecast products (ERFs and GEFS)
 286 underestimate extreme rainfall in the Narmada basin (Fig 5). The dry bias in extreme rainfall increases with lead
 287 time in the ERFs and GEFS forecasts (Fig. 5). The forecast products showed a poor correlation with the observed
 288 extreme precipitation in the Narmada river basin (Fig. 5). However, both the forecast products demonstrated
 289 relatively better skills for maximum and minimum temperatures than precipitation (Fig. S3 and S4).



290

291 **Figure 4. Comparison of the precipitation forecast skills from ERF5 and GEFS for the summer monsoon period**
 292 **during 2019-2020. Forecast skills were evaluated using bias, NRMSE, and correlation for each ensemble member of**
 293 **ERF5 and GEFS and the median skill is presented.**



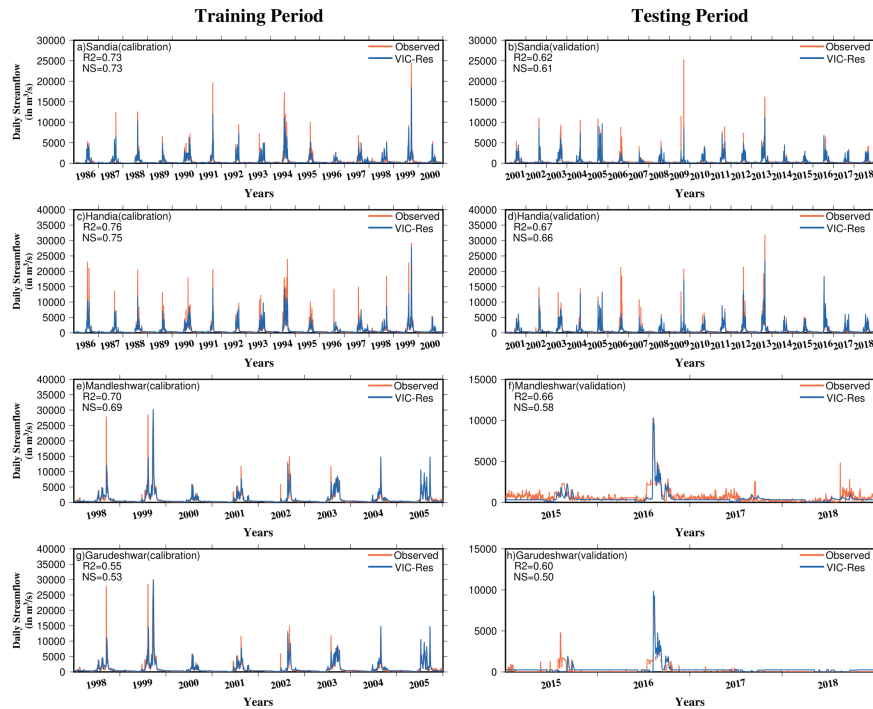
294

295 Figure 5. Comparison of the extreme precipitation (exceeding 75th percentile) forecast skills from ERF5 and GEFS for
 296 the summer monsoon period during 2019-2020. Forecast skills were evaluated using bias, NRMSE, and correlation
 297 for each ensemble member of ERF5 and GEFS and the median skill is presented.

298

299 **3.2 Calibration and evaluation of the VIC-Res model**

300 We performed calibration of reservoir level and storage and calibration of daily streamflow. Daily storage and
301 water level calibrated the VIC-Res model for four major reservoirs (Bargi, Tawa, Indira Sagar and Sardar Sarovar)
302 in the Narmada basin. The upstream catchment area of all the gauge locations and calibration parameters are shown
303 in supplementary Figure S5. We evaluated the VIC-Res model's performance using the coefficient of
304 determination (R^2) and Nash Sutcliffe Efficiency (NSE) (Fig. 6). The VIC-Res model simulates daily streamflow
305 at the selected stations in the basin. R^2 and NSE values were above 0.65 at Sandia, Handia, and Mandleshwar
306 stations for the calibration period. While at Garudeshwar, the VIC-Res model performed comparatively weaker
307 ($R^2 = 0.55$ & $NSE = 0.53$) for the calibration period.



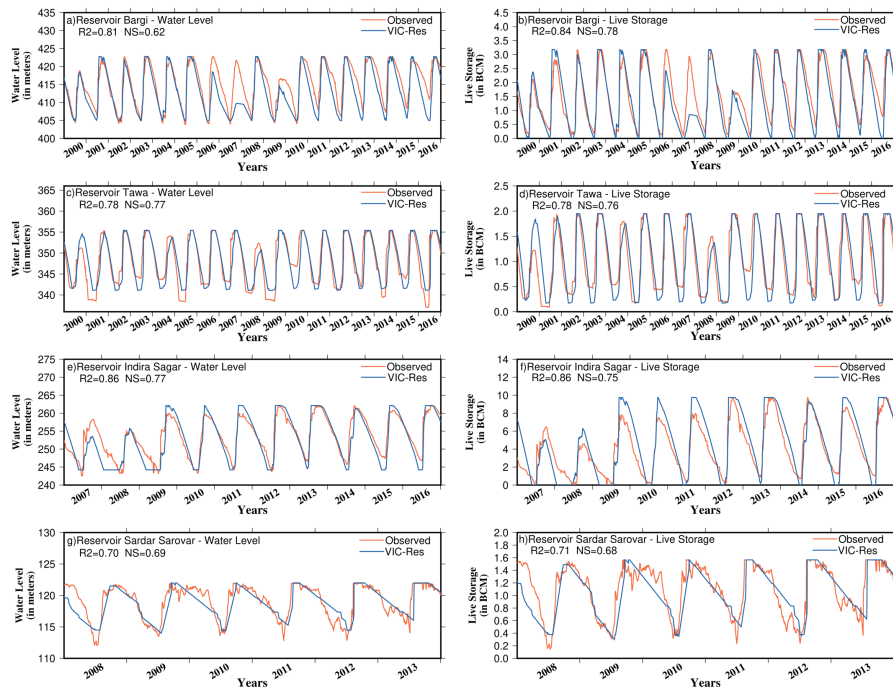
308

309 **Figure 6. Calibration and evaluation of the VIC-Res model against observed daily streamflow at gauge stations at**
 310 **Sandia, Handia, Mandleshwar and Garudeshwar. The performance of the VIC-Res model in simulating daily**
 311 **streamflow was evaluated using the R^2 and NSE.**

312

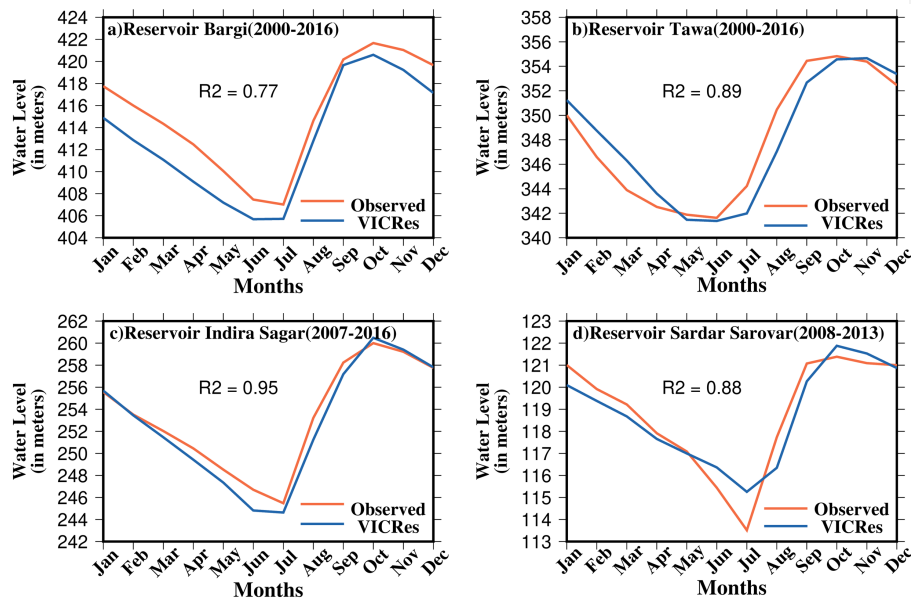
313 We considered the influence of major reservoirs on the simulated daily streamflow. Therefore, the VIC-Res
 314 model's performance in simulating daily reservoir storage and the water level was evaluated against the streamflow
 315 observations. We selected 2000-2016, 2000-2016, 2007-2016, and 2008-2013 as evaluation periods for Bargi,
 316 Tawa, Indira Sagar, and Sardar Sarovar reservoirs, respectively, based on the availability of observations. We
 317 estimated R^2 and NSE to evaluate the model's performance (Fig. 7). The model performed well in simulating all
 318 the reservoirs' water levels and storage ($R^2 > 0.78$ and $NSE > 0.62$). We also compared the seasonal cycle of the
 319 observed and simulated reservoir storage for all the four major reservoirs (Fig. 8). The model simulated monthly
 320 seasonal cycle of reservoir storage compares well with the observed storage for all the dams with R^2 of more than
 321 0.77. We find that the model underestimates storage for Bargi reservoir, which can be due to relatively smaller

322 upstream catchment area that may not capture the spatial variability of rainfall. Overall, we find that the VIC-Res
323 model can evaluate the ensemble streamflow forecast in the Narmada river basin.



324

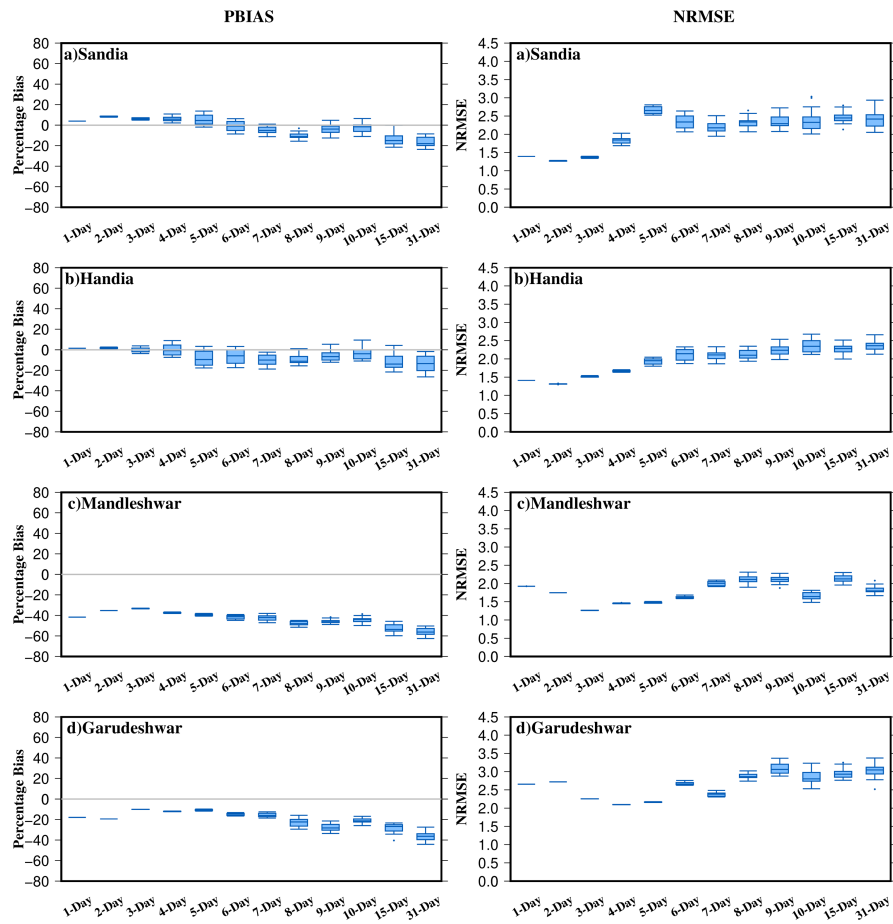
325 **Figure 7. Evaluation of the VIC-Res model in simulating daily water level and daily live storage at four major**
326 **reservoirs Bargi, Tawa, Indira Sagar and Sardar Sarovar.**



328 Figure 8. Comparison of observed and the VIC-Res model simulated reservoir water levels for four reservoirs in
 329 Narmada River basin.

330 3.3 Evaluation of ensemble streamflow forecast skills of ERFs

331 We estimated forecast skills of daily streamflow for 2003-2018 generated from each ensemble member of ERFs
 332 for the twelve lead times (1-day to 10-day, 15-day, and 31-day). We selected a 1-10 day lead as GEFS forecast is
 333 also available with the same lead. In addition, two other lead times (15 and 31 days) were selected to evaluate the
 334 forecast skill of streamflow forecast from all the sixteen members of ERFs (Fig. 9). Both bias and NRMSE showed
 335 a relatively lesser spread for the shorter lead (1-3 day) streamflow forecast from all the ensemble members of
 336 ERFs (Fig. 9). However, uncertainty in streamflow forecast due to different ensemble members increases with the
 337 lead time. NRMSE of streamflow forecast from ERFs also rises with the lead at all the stations. Ensemble
 338 streamflow forecast from ERFs showed a positive bias for Sandia, Handia, and Garudeshwar, while a negative
 339 bias was found for Mandleshwar station (Fig. 9). We estimated the CRPS, which is higher for 1-day lead compared
 340 to 3-day leads and increases with the lead time (Figure S6).



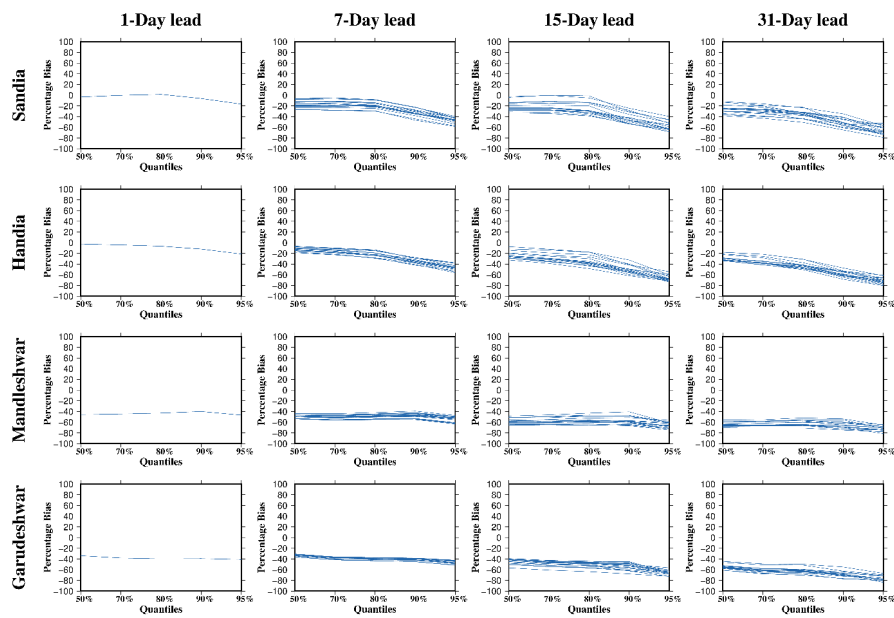
341

342 **Figure 9. Ensemble streamflow forecast skill based on the ERF5 forecast for 2003-2018. The forecast was evaluated**
 343 **using bias (%) and NRMSE. Box and whisker plots show the skill for all 16 ensemble members at lead 1-10 day, 15**
 344 **day and 31 days at four gauge stations.**

345

346 We estimated the forecast skill in streamflow exceeding certain thresholds (50,70,80,90, and 95th percentiles) [Fig.
 347 10]. We find less spread in bias among different ensemble members for 1-day lead streamflow forecast from ERF5.
 348 However, the spread of bias in streamflow forecast due to different ensemble members increases with the lead

349 time (Fig. 10). Moreover, bias in streamflow forecast remains stable for all the selected percentile thresholds at a
 350 1-day lead at all the four-gauge stations. On the other hand, bias in streamflow forecast increases for higher
 351 percentiles at longer lead times. For instance, dry bias in streamflow forecast in all the ensemble members is higher
 352 for the 95th percentile than for the 50th percentile. Therefore, our results show that regardless of the spread among
 353 the ensemble members from ERFs, almost all the ensemble members underestimate the high flow at all the gauge
 354 stations in the Narmada river basin (Fig. 10).

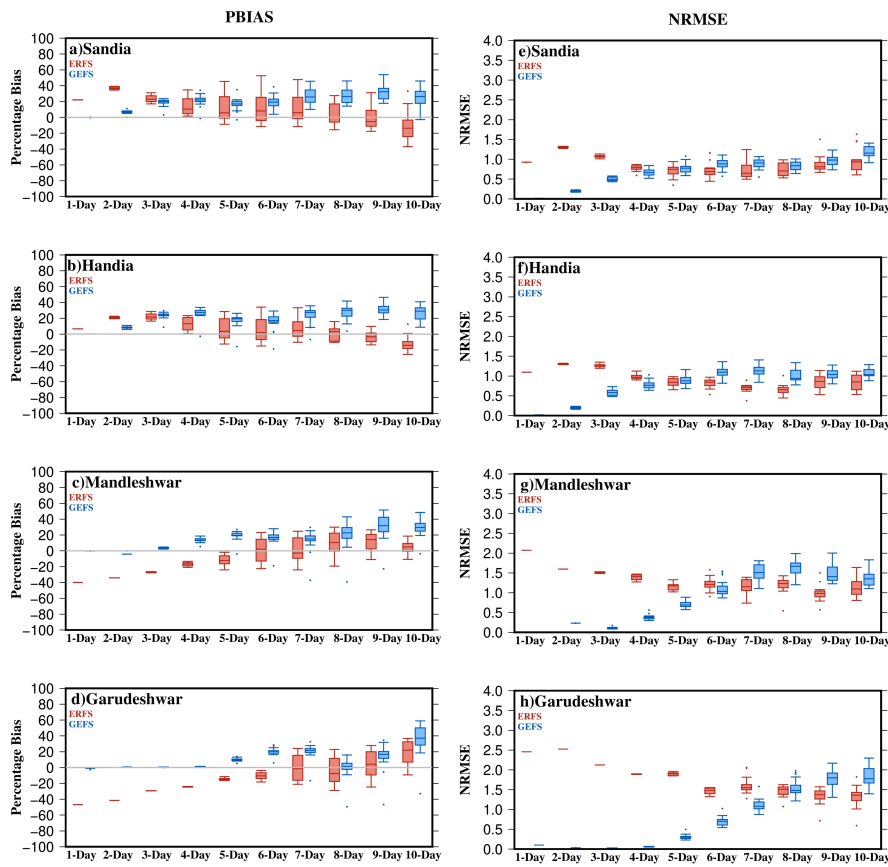


355
 356 **Figure 10.** Bias in ensemble streamflow forecast estimated using ERFs for 2003-2018 for streamflow percentiles
 357 exceeding 50th, 70th, 80th, 90th, and 95th thresholds. Bias in ensemble streamflow forecast was evaluated at 1, 7, 15, and
 358 31 day lead.

359 3.4 Comparison of ensemble streamflow forecast skills ERFs and GEFS

360 We compared the streamflow forecast skills of 16 ensemble members from ERFs and 21 ensemble members from
 361 GEFS. Since GEFS meteorological forecast is available only for 2019-2020, we compared the summer monsoon
 362 season of these two years. ERFs forecast is available weekly for 1-32 days, while the GEFS forecast is generated
 363 every day. Therefore, we compared the daily streamflow forecast from both the products for the weeks for which
 364 the ERFs forecast was available for the summer monsoon of the 2019-2020 period. We compared the streamflow
 365 forecast skills for all the ensemble members at 1 to 10 day leads at Sandia, Handia, Mandleshwar, and Garudeshwar

366 (Fig. 11). We find that the GEFS forecast has a better skill for the short lead time (~1-5 days) with less bias and
 367 NRMSE. On the other hand, the ERFs ensemble forecast showed higher bias and NRMSE at shorter leads for
 368 most of the selected locations in the Narmada basin. Streamflow forecast skill of GEFS declines rapidly after the
 369 3-4 day lead time for most of the locations in the Narmada basin. The forecast products showed a larger spread
 370 among the streamflow forecast ensemble members after five days lead. For short to medium range (~1 to 5 days),
 371 the streamflow forecast from GEFS performed better with low NRMSE and bias for streamflow exceeding the
 372 75th percentile of the summer monsoon period (Fig. S7). Moreover, streamflow forecast skill from the ERFs was
 373 considerably lower than the GEFS at most of the locations for flow exceeding 75th percentiles (Fig. S7).

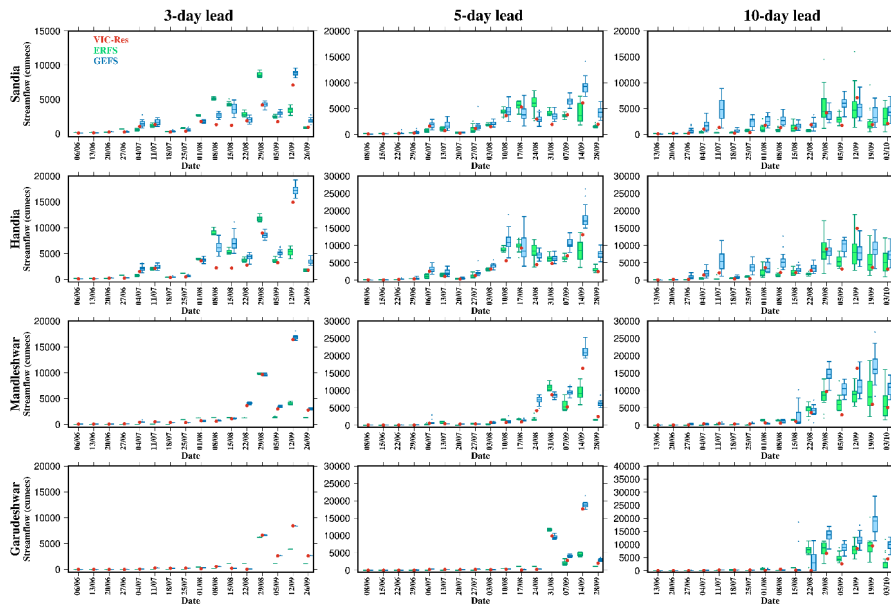


374

375 **Figure 11. Comparison of ensemble streamflow forecast skills from ERFs and GEFS for 2019-2020. The forecast skill**
 376 **was evaluated considering the VIC-Res simulated streamflow with the observed forcing from IMD due to**
 377 **unavailability of observed flow.**

378 We examined the daily streamflow forecast skill at 3-day, 5-day, and 10-leads from ERFs and GEFS forecasts for
 379 the summer monsoon season of 2019 & 2020 against VIC-Res simulated streamflow using the observed
 380 meteorological forcing at all the four gauge stations (Fig. 12 and Fig. S8). Since observed daily streamflow was
 381 unavailable for skill assessment, the comparison was made against the VIC model simulated flow with the
 382 observed meteorological forcing (Fig. 12 and Fig. S8). The GEFS forecast successfully captured streamflow peaks
 383 in both 2019 and 2020 at a 3-day lead. In 2019, GEFS forecasts overestimated streamflow peaks at 3-day and 5-
 384 day leads during the summer monsoon. On the other hand, the ensemble streamflow forecast developed using the
 385 ERFs meteorological forecast showed a higher spread than GEFS (Fig. 12, Fig. S8). The spread in ensemble
 386 streamflow forecast increases for both ERFs and GEFS forecast at a 10-day lead. However, the ERFs's streamflow
 387 forecast showed a better skill at the 10-day lead. Despite having fewer ensemble members than the GEFS, the
 388 ERFs forecast showed a broader spread in streamflow prediction, highlighting a higher uncertainty in prediction.
 389 We find that GEFS overestimate streamflow the ERFs underestimates most of the locations and lead times.

390

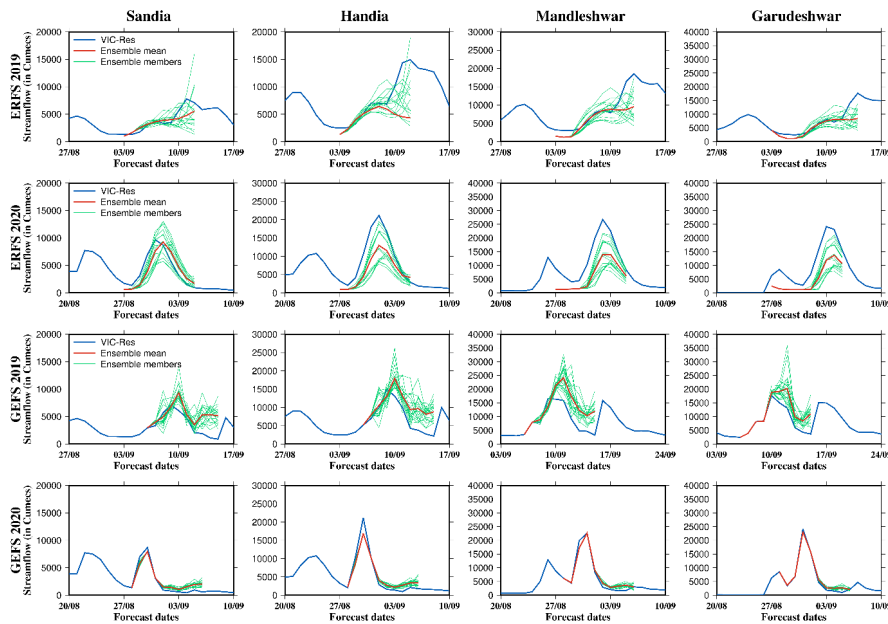


391

392 **Figure 12. Comparison of ensemble streamflow simulated using the VIC-Res model with ERFs and GEFS forecast**
 393 **products during the summer monsoon of 2019. The forecast skill was evaluated considering the VIC-Res simulated**
 394 **streamflow with the observed forcing from IMD due to unavailability of observed flow.**

395

396 We examined the streamflow forecast generated by all the ensemble members of ERFs and GEFS for a few events
 397 using the VIC-Res model (Fig. 13). The ensemble streamflow prediction was compared considering the model
 398 simulated streamflow with the observed forcing from IMD. In 2019, the ensemble mean streamflow from all the
 399 ensemble members of ERFs considerably underestimated the peak flow (Fig. 13). However, a few ensemble
 400 members of the ERFs forecast captured the peak flow at the four locations of the Narmada river basin (Fig. 13).
 401 At Handia station, 1 out of 16 ensemble members exceeds the observed streamflow. Moreover, GEFS forecasts at
 402 short leads (3-5 days) performed well in capturing peaks (Fig. 13). However, GEFS forecasts showed a smaller
 403 spread in ensemble streamflow at the short lead time (1-5 days). Overall, we find that ensemble forecasts can be
 404 used for probabilistic streamflow prediction.



405

406 **Figure 13. Ensemble streamflow simulations using the ERFs forecast at 5-11 day lead and GEFS forecast at 3-5 day**
 407 **lead against the VIC-Res simulated streamflow with the observed meteorological forcing for 2019 and 2020.**

409 4 Discussion and conclusions

410 Streamflow forecast plays an essential role in efficient reservoir operations and flood mitigation (Chen et al., 2016;
411 Mediero et al., 2007). A reliable streamflow forecast can reduce uncertainty in reservoir operations and enhance
412 the development of a flood early warning system. Notwithstanding the considerable progress in an operational
413 meteorological forecast from different agencies, efforts to establish an ensemble streamflow forecast system at
414 river basin scales have been limited for India. Moreover, it remains unclear if other meteorological forecast
415 products have different streamflow forecast skills. We used the two meteorological ensemble forecast products
416 from IMD to examine streamflow forecast skills in the Narmada river basin. The presence of reservoirs influence
417 the water budget and streamflow (Shah et al., 2019; Zajac et al., 2017; Yun et al., 2020; Chai et al., 2019).
418 Hydrological model parameters calibrated without considering the role of reservoirs can be erroneous and leading
419 to errors and uncertainty in simulated hydrological processes (Dang et al., 2019). Therefore, we used the ensemble
420 streamflow prediction approach to generate the daily streamflow simulations considering the influence of
421 reservoirs in the Narmada river basin. We compared the performance of ERFs and GEFS ensembles for the
422 summer monsoon period of 2019-20. We also assessed the skills of the ERFs dataset solely for a more extended
423 period from 2003 to 2018.

424 The ERFs ensemble forecast is available once a week at 1-32 days lead time. On the other hand, GEFS ensemble
425 forecasts are available daily at 1-10 days lead for the summer monsoon period of 2019-2020. Hagedorn et al.
426 (2005) reported that bias-correction of the raw forecast does not necessarily increase the forecast skill. Moreover,
427 statistical correction of the raw forecast is inappropriate, which can lose its effect propagating through the
428 hydrological model (Zalachori et al., 2012; Crochemore et al., 2016; Benninga et al., 2017; Hagedorn et al., 2005).
429 Therefore, we did not bias-correct the raw meteorological ensemble forecasts from ERFs and GEFS. The skills of
430 ERFs and GEFS precipitation and temperature (minimum and maximum) forecasts were estimated for 1-, 5- and
431 10-day lead. The GEFS raw forecast showed better skills than the ERFs forecast for mean and extreme
432 precipitation. As precipitation plays a vital role in streamflow forecast (Meaurio et al., 2017; Demargne et al.,
433 2014; Pappenberger et al., 2005), our results show that GEFS forecast provides better skills for streamflow
434 prediction in the Narmada River basin. The post-processing of streamflow data can significantly improve
435 performance (Tiwari et al., 2021; Muhammad et al., 2018), which can be used in the future to examine the
436 improvements in streamflow prediction. Moreover, a multi-model approach can be used to reduce the errors and
437 uncertainty in streamflow forecasts that could arise due to the parameterization of hydrological models (Velázquez
438 et al., 2011; Zarzar et al., 2018; Muhammad et al., 2018).

439 The skills of ERFs and GEFS ensemble forecasts were estimated for 1, 5 and 10-day leads. GEFS raw forecasts
440 illustrated better skills than ERFs forecasts for overall rainfall and extreme precipitation. As studies show that rain
441 plays a vital role in streamflow forecast (Demargne et al., 2014; Meaurio et al., 2017; Pappenberger et al., 2005),

Deleted: hydrologic

443 we also observed the same results. The ensemble forecast with better skills performed well in predicting daily
444 streamflow. Correcting the bias of the input forecast may shrink the variability range of the result. However,
445 ensemble forecasts aim to capture uncertainties. Studies suggest that the post-processing of streamflow data can
446 significantly improve performance (Muhammad et al., 2018; Tiwari et al., 2021). A multi-model approach, where
447 more than one hydrological model is used, can generalize the uncertainty introduced by the hydrological model.
448 Various studies have reported improved forecast skills using the multi-model approach (Muhammad et al., 2018;
449 Velázquez et al., 2011; Zarzar et al., 2018). Also, our analysis is based on just for the 2019-2020 as the GEFS
450 hindcast is available only for this period. Availability of longer hindcast from the GEFS can help to understand
451 the forecast skills for hydrological extremes (drought and floods). Moreover, we did not examine the forecast skill
452 of reservoir storage, which can provide a better understanding of the impacts of storage during the floods.

Deleted: hydrologic

Deleted: hydrologic

Deleted: hydrologic

453 Flood forecasting using the available meteorological forecast products can help in mitigating the losses through
454 early warnings. To account for the uncertainty arising from initial state and model parameterization, the individual
455 members of the ensemble weather forecast can provide better information than their ensemble mean (Saleh et al.,
456 2019). The probabilistic approach over the deterministic method provides the range of variability, which can help
457 determine the probability of exceeding a specific threshold of streamflow (Hsiao et al., 2013). The shift from the
458 existing 'flood forecast system' to the 'ensemble-based probabilistic forecast' requires modifications in the current
459 flood forecast practice. The transition is expected to change various aspects of the existing decision-making
460 process. The forecasters need to train the on-duty officers adequately and the authorities on probabilistic forecasts.
461 We evaluated the streamflow forecast skills at 1-32 day lead in the Narmada river basin. The increased lead time
462 in streamflow forecast can assist in developing efficient communication methods of information (Arnal et al.,
463 2020; Ramos et al., 2010). Moreover, ensemble streamflow forecast at longer leads can be effectively used in
464 optimizing reservoir operations (Alemu et al., 2011). Our results show that, while the mean of the ensemble
465 members failed to capture the high flows, a few individual ensemble members performed better in capturing peak
466 flow, which can be used to develop probabilistic early warnings.

467 Based on our findings, the following conclusions can be made:

- 468 1) The raw precipitation forecast from both GEFS and ERFS datasets showed moderate skills (bias, NRMSE
469 and correlation) against observations from IMD at 1-day, 5-day and 10-day lead times. While both (ERFS
470 and GEFS) forecast products underestimated extreme precipitation, dry bias in the ERFS forecast was
471 more prominent than the GEFS forecast. For instance, raw precipitation forecast from ERFS showed
472 negative bias across the Narmada river basin. On the other hand, the raw precipitation forecast from GEFS
473 exhibited both negative and positive bias. Both the forecast products showed better skills for maximum
474 and minimum temperatures than precipitation.
- 475 2) We calibrated and evaluated the VIC-Res model to simulate streamflow, considering the influence of
476 reservoirs at four gauge stations in the Narmada River Basin. The model reproduced daily streamflow,
477 reservoir water level, and storage reasonably well against the observations.

481 3) Comparing the streamflow forecast skills of both the ensemble forecasts showed that GEFS forecasts
482 performed better than the ERFs at all the locations in the basin. However, both the forecast products
483 underestimated the extremes, which can be due to dry bias in extreme precipitation. The spread in
484 streamflow due to different ensemble members increased with the forecast lead time. Overall, an
485 ensemble forecast can be used to develop a probabilistic forecast based flood early warning system.

486 **Data availability:** All the datasets used in this study can be obtained from the corresponding author.

487

488 **Competing interest:** Authors declare no competing interest.

489 **Author contributions:** VM designed the study. UV conducted simulations and wrote the first draft. UV and
490 VM discussed the results and prepared the final version.

491 **Acknowledgement:** The work was supported by the Monsoon Mission, Ministry of Earth Sciences. The authors
492 acknowledge the data availability from India Meteorological Department (IMD) and India-WRIS. ERFs and
493 GEFS forecast products were obtained from the Indian Institute of Tropical Meteorology (IITM), Pune.

494 **References**

- 495 Alemu, E. T., Palmer, R. N., Polebitski, A., and Meaker, B.: Decision Support System for Optimizing Reservoir
496 Operations Using Ensemble Streamflow Predictions, *J Water Resour Plan Manag*, 137, 72–82,
497 [https://doi.org/10.1061/\(asce\)wr.1943-5452.0000088](https://doi.org/10.1061/(asce)wr.1943-5452.0000088), 2011.
- 498 Alfieri, L., Burek, P., Dutra, E., Krzeminski, B., Muraro, D., Thielen, J., and Pappenberger, F.: GloFAS-global
499 ensemble streamflow forecasting and flood early warning, *Hydrol Earth Syst Sci*, 17, 1161–1175,
500 <https://doi.org/10.5194/hess-17-1161-2013>, 2013.
- 501 Ali, H., Modi, P., and Mishra, V.: Increased flood risk in Indian sub-continent under the warming climate,
502 *Weather Clim Extrem*, 25, <https://doi.org/10.1016/j.wace.2019.100212>, 2019.
- 503 Arnal, L., Anspoks, L., Manson, S., Neumann, J., Norton, T., Stephens, E., Wolfenden, L., and Cloke, H. L.: “
504 Are we talking just a bit of water out of bank ? Or is it Armageddon ?” Front line perspectives on transitioning to
505 probabilistic fluvial flood forecasts in England, 203–232, <https://doi.org/https://doi.org/10.5194/gc-3-203-2020>,
506 2020.
- 507 Benninga, H. F., Booij, M. J., Romanowicz, R. J., and Rientjes, T. H. M.: Performance of ensemble streamflow
508 forecasts under varied hydrometeorological conditions, 5273–5291, <https://doi.org/https://doi.org/10.5194/hess-21-5273-2017>, 2017.
- 509
- 510 Boulange Julien and Hanasaki Naota: A global flood risk analysis with explicit representation of major dams,
511 https://doi.org/https://doi.org/10.11520/jshwr.32.0_12, 2013.
- 512 Bowler, N. E., Arribas, A., Mylne, K. R., Robertson, K. B., and Beare, S. E.: The MOGREPS short-range
513 ensemble prediction system, 722, 703–722, <https://doi.org/10.1002/qj>, 2008.
- 514 Chai, Y., Li, Y., Yang, Y., Zhu, B., Li, S., Xu, C., and Liu, C.: Influence of Climate Variability and Reservoir
515 Operation on Streamflow in the Yangtze River, *Sci Rep*, 9, <https://doi.org/10.1038/s41598-019-41583-6>, 2019.

516 Chen, L., Singh, V. P., Lu, W., Zhang, J., Zhou, J., and Guo, S.: Streamflow forecast uncertainty evolution and
517 its effect on real-time reservoir operation, *J Hydrol (Amst)*, 540, 712–726,
518 <https://doi.org/10.1016/j.jhydrol.2016.06.015>, 2016.

519 Cloke, H. L. and Pappenberger, F.: Ensemble flood forecasting : A review, *J Hydrol (Amst)*, 375, 613–626,
520 <https://doi.org/10.1016/j.jhydrol.2009.06.005>, 2009.

521 Crochemore, L., Ramos, M. H., and Pappenberger, F.: Bias correcting precipitation forecasts to improve the skill
522 of seasonal streamflow forecasts, *Hydrol Earth Syst Sci*, 20, 3601–3618, [https://doi.org/10.5194/hess-20-3601-](https://doi.org/10.5194/hess-20-3601-2016)
523 2016, 2016.

524 Dang, T. D., Chowdhury, A. K., and Galelli, S.: On the representation of water reservoir storage and operations
525 in large-scale hydrological models: implications on model parameterization and climate change impact
526 assessments, *Hydrology and Earth System Sciences Discussions*, 1–34, <https://doi.org/10.5194/hess-2019-334>,
527 2019.

528 Dang, T. D., Vu, D. T., Chowdhury, A. F. M. K., and Galelli, S.: A software package for the representation and
529 optimization of water reservoir operations in the VIC hydrologic model, *Environmental Modelling and Software*,
530 126, 104673, <https://doi.org/10.1016/j.envsoft.2020.104673>, 2020.

531 Dawson, C. W., Abrahart, R. J., and See, L. M.: HydroTest : A web-based toolbox of evaluation metrics for the
532 standardised assessment of hydrological forecasts, 22, 1034–1052, <https://doi.org/10.1016/j.envsoft.2006.06.008>,
533 2007.

534 Demargne, J., Wu, L., Regonda, S. K., Brown, J. D., Lee, H., He, M., Seo, D. J., Hartman, R., Herr, H. D.,
535 Fresch, M., Schaake, J., and Zhu, Y.: The science of NOAA’s operational hydrologic ensemble forecast service,
536 *Bull Am Meteorol Soc*, 95, 79–98, <https://doi.org/10.1175/BAMS-D-12-00081.1>, 2014.

537 Demeritt, D., Pappenberger, F., Centre, E., Weather, R., and Rg, R.: Challenges in communicating and using
538 ensembles in operational flood forecasting, 222, 209–222, <https://doi.org/10.1002/met.194>, 2010.

539 Dipti, J.: What is the impact of floods on India’s GDP?,
540 [https://www.livemint.com/Politics/M1cZ2bfYHSG7yCdHHvUozN/Are-floods-causing-more-damage-these-](https://www.livemint.com/Politics/M1cZ2bfYHSG7yCdHHvUozN/Are-floods-causing-more-damage-these-days.html)
541 days.html, 2017.

542 Dong, N., Wei, J., Yang, M., Yan, D., Yang, C., Gao, H., Arnault, J., Laux, P., Zhang, X., Liu, Y., Niu, J.,
543 Wang, H., Wang, H., Kunstmann, H., and Yu, Z.: Model Estimates of China’s Terrestrial Water Storage
544 Variation Due To Reservoir Operation, *Water Resour Res*, 58, <https://doi.org/10.1029/2021WR031787>, 2022.

545 Field, C. B., Barros, V., Stocker, T. F., Dahe, Q., Dokken, D. J., Ebi, K. L., Mastrandrea, M. D., Pauline, K. J.
546 M., Plattner, G.-K., Allen, S. K., Tignor, M., and Midgley, P. M.: Special Report of the Intergovernmental Panel
547 on Climate Change Edited, 30 pp., 2011.

548 Gain, A. K. and Giupponi, C.: Impact of the Farakka Dam on thresholds of the hydrologic: Flow regime in the
549 Lower Ganges River Basin (Bangladesh), *Water (Switzerland)*, 6, 2501–2518,
550 <https://doi.org/10.3390/w6082501>, 2014.

551 Gao, H., Tang, Q., Shi, X., Zhu, C., Bohn, T., and Su, F.: Water Budget Record from Variable Infiltration
552 Capacity (VIC) Model, 120–173 pp., 2009.

Deleted: hydrological

Deleted: hydrological

555 Georgakakos, A. P., Yao, H., Kistenmacher, M., Georgakakos, K. P., Graham, N. E., Cheng, F. Y., Spencer, C.,
556 and Shamir, E.: Value of adaptive water resources management in Northern California under climatic variability
557 and change: Reservoir management, *J Hydrol (Amst)*, 412–413, 34–46,
558 <https://doi.org/10.1016/j.jhydrol.2011.04.038>, 2012.

559 Gneiting, T. and Raftery, A. E.: Strictly Proper Scoring Rules, Prediction, and Estimation, *J Am Stat Assoc*, 102,
560 359–378, <https://doi.org/10.1198/016214506000001437>, 2007.

561 Gosain, A. K., Rao, S., and Basuray, D.: Climate change impact assessment on hydrology of Indian river basins,
562 346–353 pp., 2006.

563 Goswami, S. B., Bal, P. K., and Mitra, A. K.: Use of rainfall forecast from a high-resolution global NWP model
564 in a hydrological stream flow model over Narmada river basin during monsoon, *Model Earth Syst Environ*, 4,
565 1029–1040, <https://doi.org/10.1007/s40808-018-0436-y>, 2018.

566 Hagedorn, R., Doblas-Reyes, F. J., and Palmer, T. N.: The rationale behind the success of multi-model
567 ensembles in seasonal forecasting — I. Basic concept, *Tellus A: Dynamic Meteorology and Oceanography*, 57,
568 219–233, <https://doi.org/10.3402/tellusa.v57i3.14657>, 2005.

569 Hanasaki, N., Yoshikawa, S., Pokhrel, Y., and Kanae, S.: A global hydrological simulation to specify the sources
570 of water used by humans, *Hydrol Earth Syst Sci*, 22, 789–817, <https://doi.org/10.5194/hess-22-789-2018>, 2018.

571 Harsha, J.: Fighting floods with insufficient warning, [https://www.thestatesman.com/opinion/fighting-floods-](https://www.thestatesman.com/opinion/fighting-floods-insufficient-warning-1502924062.html)
572 [insufficient-warning-1502924062.html](https://www.thestatesman.com/opinion/fighting-floods-insufficient-warning-1502924062.html), 2020a.

573 Harsha, J.: Playing catch up in flood forecasting technology, [https://www.thehindu.com/opinion/lead/playing-](https://www.thehindu.com/opinion/lead/playing-catch-up-in-flood-forecasting-technology/article32797281.ece)
574 [catch-up-in-flood-forecasting-technology/article32797281.ece](https://www.thehindu.com/opinion/lead/playing-catch-up-in-flood-forecasting-technology/article32797281.ece), 2020b.

575 Hersbach, H.: Decomposition of the Continuous Ranked Probability Score for Ensemble Prediction Systems,
576 2000.

577 Hsiao, L. F., Yang, M. J., Lee, C. S., Kuo, H. C., Shih, D. S., Tsai, C. C., Wang, C. J., Chang, L. Y., Chen, D. Y.
578 C., Feng, L., Hong, J. S., Fong, C. T., Chen, D. S., Yeh, T. C., Huang, C. Y., Guo, W. D., and Lin, G. F.:
579 Ensemble forecasting of typhoon rainfall and floods over a mountainous watershed in Taiwan, *J Hydrol (Amst)*,
580 506, 55–68, <https://doi.org/10.1016/j.jhydrol.2013.08.046>, 2013.

581 Jain, S. K., Mani, P., Jain, S. K., Prakash, P., Vijay, P., Tullios, D., Kumar, S., Agarwal, S. P., and Dimri, A. P.:
582 A Brief review of flood forecasting techniques and their applications, *Intl. J. River Basin Management*, 0, 1–16,
583 <https://doi.org/10.1080/15715124.2017.1411920>, 2018.

584 Jarvis, A.: Hole-field seamless SRTM data, International Centre for Tropical Agriculture (CIAT), 2008.

585 Joshi, H.: Floods across the country highlight need for a robust flood management structure,
586 [https://india.mongabay.com/2020/08/floods-across-the-country-highlight-need-for-a-robust-flood-management-](https://india.mongabay.com/2020/08/floods-across-the-country-highlight-need-for-a-robust-flood-management-structure/)
587 [structure/](https://india.mongabay.com/2020/08/floods-across-the-country-highlight-need-for-a-robust-flood-management-structure/), 2020.

588 Krzysztofowicz, R.: The case for probabilistic forecasting in hydrology, 249, 2–9,
589 [https://doi.org/https://doi.org/10.1016/S0022-1694\(01\)00420-6](https://doi.org/https://doi.org/10.1016/S0022-1694(01)00420-6), 2001.

590 Liang, X., Lettenmaier, D. P., Wood, E. F., and Burges, S. J.: A simple hydrologically based model of land
591 surface water and energy fluxes for general circulation models, *Journal of Geophysical Research: Atmospheres*,
592 99, 14415–14428, <https://doi.org/10.1029/94JD00483>, 1994.

593 Luo, T., Maddocks, A., Iceland, C., Ward, P., and Winsemius, H.: World's 15 countries with the most people
594 exposed to river floods., <https://www.wri.org/insights/worlds-15-countries-most-people-exposed-river-floods>,
595 2015.

596 Madhusoodhanan, C. G., Sreeja, K. G., and Eldho, T. I.: Climate change impact assessments on the water
597 resources of India under extensive human interventions, *Ambio*, 45, 725–741, <https://doi.org/10.1007/s13280-016-0784-7>, 2016.

599 Meaurio, M., Zabaleta, A., Boithias, L., Epelde, A. M., Sauvage, S., Sánchez-Pérez, J. M., Srinivasan, R., and
600 Antigüedad, I.: Assessing the hydrological response from an ensemble of CMIP5 climate projections in the
601 transition zone of the Atlantic region (Bay of Biscay), *J Hydrol (Amst)*, 548, 46–62,
602 <https://doi.org/10.1016/j.jhydrol.2017.02.029>, 2017.

603 Mediero, L., Garrote, L., and Martín-Carrasco, F.: A probabilistic model to support reservoir operation decisions
604 during flash floods, *Hydrological Sciences Journal*, 52, 523–537, <https://doi.org/10.1623/hysj.52.3.523>, 2007.

605 Mishra, V., Cherkauer, K. A., Niyogi, D., Lei, M., Pijanowski, B. C., Ray, D. K., Bowling, L. C., and Yang, G.:
606 A regional scale assessment of land use/land cover and climatic changes on water and energy cycle in the upper
607 Midwest United States, *International Journal of Climatology*, 30, 2025–2044, <https://doi.org/10.1002/joc.2095>,
608 2010.

609 Muhammad, A., Stadnyk, T. A., Unduche, F., and Coulibaly, P.: Multi-model approaches for improving
610 seasonal ensemble streamflow prediction scheme with various statistical post-processing techniques in the
611 Canadian Prairie Region, *Water (Switzerland)*, 10, <https://doi.org/10.3390/w10111604>, 2018.

612 Mukhopadhyay, P., Krishna, R. P. M., Deshpande, M., Ganai, M., Tirkey, S., Goswami, T., and Sarkar, S.: High
613 Resolution (12 . 5 km) Ensemble Prediction system based on GEFS : Evaluation of extreme precipitation events
614 over Indian region, 2–4, 2018.

615 Nanditha, J. S. and Mishra, V.: On the need of ensemble flood forecast in India, *Water Secur*, 12, 100086,
616 <https://doi.org/10.1016/j.wasec.2021.100086>, 2021.

617 Nanditha, J. S. and Mishra, V.: Multiday Precipitation Is a Prominent Driver of Floods in Indian River Basins,
618 *Water Resour Res*, 58, e2022WR032723, <https://doi.org/https://doi.org/10.1029/2022WR032723>, 2022.

619 Nash, J. E. and Sutcliffe, J. V.: RIVER FLOW FORECASTING THROUGH CONCEPTUAL MODELS PART
620 I - A DISCUSSION OF PRINCIPLES*, *J Hydrol (Amst)*, 10, 282–290, 1970.

621 Pai, D. S., Sridhar, L., Rajeevan, M., Sreejith, O. P., Satbhai, N. S., and Mukhopadhyay, B.: (1901-2010) daily
622 gridded rainfall data set over India and its comparison with existing data sets over the region, *Mausam*, 1, 1–18,
623 2014.

624 Pai, D. S., Sridhar, L., Badwaik, M. R., and Rajeevan, M.: Analysis of the daily rainfall events over India using a
625 new long period (1901–2010) high resolution ($0.25^\circ \times 0.25^\circ$) gridded rainfall data set, *Clim Dyn*, 45, 755–776,
626 <https://doi.org/10.1007/s00382-014-2307-1>, 2015.

- 627 Pappenberger, F., Beven, K. J., Hunter, N. M., Bates, P. D., Gouweleeuw, B. T., Thielen, J., and de Roo, A. P.
 628 J.: Cascading model uncertainty from medium range weather forecasts (10 days) through a rainfall-runoff model
 629 to flood inundation predictions within the European Flood Forecasting System (EFFS), *Hydrol Earth Syst Sci*, 9,
 630 381–393, <https://doi.org/10.5194/hess-9-381-2005>, 2005.
- 631 Pappenberger, F., Stephens, E., Thielen, J., Salamon, P., Demeritt, D., Jan, S., Wetterhall, F., and Al, L.:
 632 Visualizing probabilistic flood forecast information: expert preferences and perceptions of best practice in
 633 uncertainty communication, <https://doi.org/10.1002/hyp>, 2012.
- 634 Ramos, M. H., Mathevet, T., Thielen, J., and Pappenberger, F.: Communicating uncertainty in hydro-
 635 meteorological forecasts: Mission impossible?, *Meteorological Applications*, 17, 223–235,
 636 <https://doi.org/10.1002/met.202>, 2010.
- 637 Ray, K., Pandey, P., Pandey, C., Dimri, A. P., and Kishore, K.: On the recent floods in India, *Curr Sci*, 117, 204–
 638 218, <https://doi.org/10.18520/cs/v117/i2/204-218>, 2019.
- 639 Reed, P. M., Hadka, D., Herman, J. D., Kasprzyk, J. R., and Kollat, J. B.: Evolutionary multiobjective
 640 optimization in water resources: The past, present, and future, *Adv Water Resour*, 51, 438–456,
 641 <https://doi.org/10.1016/j.advwatres.2012.01.005>, 2013.
- 642 Saleh, F., Ramaswamy, V., Georgas, N., Blumberg, A. F., and Pullen, J.: Inter-comparison between retrospective
 643 ensemble streamflow forecasts using meteorological inputs from ECMWF and NOAA/ESRL in the Hudson
 644 River sub-basins during Hurricane Irene (2011), *Hydrology Research*, 50, 166–186,
 645 <https://doi.org/10.2166/nh.2018.182>, 2019.
- 646 Shah, R., Sahai, A. K., and Mishra, V.: Short to sub-seasonal hydrologic forecast to manage water and
 647 agricultural resources in India, *Hydrol Earth Syst Sci*, 21, 707–720, <https://doi.org/10.5194/hess-21-707-2017>,
 648 2017.
- 649 Shah, H. L., Zhou, T., Sun, N., Huang, M., and Mishra, V.: Roles of Irrigation and Reservoir Operations in
 650 Modulating Terrestrial Water and Energy Budgets in the Indian Subcontinental River Basins, *Journal of*
 651 *Geophysical Research: Atmospheres*, 124, 12915–12936, <https://doi.org/10.1029/2019JD031059>, 2019.
- 652 Sharma, P. J., Patel, P. L., and Jothiprakash, V.: Impact assessment of Hathnur reservoir on hydrological regimes
 653 of Tapi River, India, *ISH Journal of Hydraulic Engineering*, 27, 433–445,
 654 <https://doi.org/10.1080/09715010.2019.1574616>, 2021.
- 655 Sheffield, J. and Wood, E. F.: Characteristics of global and regional drought, 1950–2000: Analysis of soil
 656 moisture data from off-line simulation of the terrestrial hydrologic cycle, 112, 1–21,
 657 <https://doi.org/10.1029/2006JD008288>, 2007.
- 658 Sikder, M. S. and Hossain, F.: Improving operational flood forecasting in monsoon climates with bias-corrected
 659 quantitative forecasting of precipitation, *International Journal of River Basin Management*, 17, 411–421,
 660 <https://doi.org/10.1080/15715124.2018.1476368>, 2019.
- 661 Singh, O. and Kumar, M.: Flood events, fatalities and damages in India from 1978, 1815–1834,
 662 <https://doi.org/10.1007/s11069-013-0781-0>, 2013.

Deleted: hydrological

Deleted: hydrological

665 Srivastava, A. K., Rajeevan, M., and Kshirsagar, S. R.: Development of a high resolution daily gridded
666 temperature data set (1969 – 2005) for the Indian region, *Atmospheric Science Letters*, 10, 249–254,
667 <https://doi.org/10.1002/asl>, 2009.

668 Teja, K. N. and Umamahesh, N. v: Application of Ensemble Techniques for Flood Forecasting in India, Roorkee
669 Water Conclave, 2020.

670 Tiwari, A. D., Mukhopadhyay, P., and Mishra, V.: Influence of bias correction of meteorological and streamflow
671 forecast on hydrological prediction in India, *J Hydrometeorol*, 1–60, <https://doi.org/10.1175/jhm-d-20-0235.1>,
672 2021.

673 Tiwari, A. D. and Mishra, V.: Sub-Seasonal Prediction of Drought and Streamflow Anomalies for Water
674 Management in India, *Journal of Geophysical Research: Atmospheres*, 127, e2021JD035737,
675 <https://doi.org/https://doi.org/10.1029/2021JD035737>, 2022.

676 Todini, E.: Flood Forecasting and Decision Making in the new Millennium . Where are We ?,
677 <https://doi.org/10.1007/s11269-017-1693-7>, 2017.

678 Tripathi, P.: Flood Disaster in India : An Analysis of trend and Preparedness Flood Disaster in India : An
679 Analysis of trend and Preparedness, 2016.

680 Uday Kumar, A. and Jayakumar, K. v.: Hydrological alterations due to anthropogenic activities in Krishna River
681 Basin, India, *Ecol Indic*, 108, <https://doi.org/10.1016/j.ecolind.2019.105663>, 2020.

682 Velázquez, J. A., Anctil, F., Ramos, M. H., and Perrin, C.: Can a multi-model approach improve hydrological
683 ensemble forecasting? A study on 29 French catchments using 16 hydrological model structures, *Advances in*
684 *Geosciences*, 29, 33–42, <https://doi.org/10.5194/adgeo-29-33-2011>, 2011.

685 Wu, W., Emerton, R., Duan, Q., Wood, A. W., Wetterhall, F., and Robertson, D. E.: Ensemble flood
686 forecasting : Current status and future opportunities, 1–32, <https://doi.org/10.1002/wat2.1432>, 2020.

687 Yassin, F., Razavi, S., Elshamy, M., Davison, B., Sapriza-azuri, G., and Wheeler, H.: Representation and
688 improved parameterization of reservoir operation in hydrological and land-surface models, 3735–3764,
689 <https://doi.org/https://doi.org/10.5194/hess-23-3735-2019>, 2019.

690 Yun, X., Tang, Q., Wang, J., Liu, X., Zhang, Y., Lu, H., Wang, Y., Zhang, L., and Chen, D.: Impacts of climate
691 change and reservoir operation on streamflow and flood characteristics in the Lancang-Mekong River Basin, *J*
692 *Hydrol (Amst)*, 590, <https://doi.org/10.1016/j.jhydrol.2020.125472>, 2020.

693 Zajac, Z., Revilla-romero, B., Salamon, P., Burek, P., Feyera, A., and Beck, H.: The impact of lake and reservoir
694 parameterization on global streamflow simulation, *J Hydrol (Amst)*,
695 <https://doi.org/10.1016/j.jhydrol.2017.03.022>, 2017.

696 Zalachori, I., Ramos, M.-H., Garçon, R., Mathevet, T., and Gailhard, J.: Statistical processing of forecasts for
697 hydrological ensemble prediction: a comparative study of different bias correction strategies, *Advances in*
698 *Science and Research*, 8, 135–141, <https://doi.org/10.5194/asr-8-135-2012>, 2012.

699 Zarzar, C. M., Hosseiny, H., Siddique, R., Gomez, M., Smith, V., Mejia, A., and Dyer, J.: A Hydraulic
700 MultiModel Ensemble Framework for Visualizing Flood Inundation Uncertainty, *J Am Water Resour Assoc*, 54,
701 807–819, <https://doi.org/10.1111/1752-1688.12656>, 2018.

702 Zhang, J., Chen, J., Li, X., Chen, H., Xie, P., and Li, W.: Combining Postprocessed Ensemble Weather Forecasts
703 and Multiple Hydrological Models for Ensemble Streamflow Predictions, *J Hydrol Eng*, 25, 04019060,
704 [https://doi.org/10.1061/\(asce\)he.1943-5584.0001871](https://doi.org/10.1061/(asce)he.1943-5584.0001871), 2020.

705

706